Research Square

Preprints are preliminary reports that have not undergone peer review.
They should not be considered conclusive, used to inform clinical practice,
or referenced by the media as validated information.

Deciphering key root traits involved in phosphorus deficiency tolerance of bread wheat (Triticum aestivum L.)

christophe Salon

christophe.salon@dijon.inra.fr

INRAE: Institut National de Recherche pour l'Agriculture l'Alimentation et l'Environnement
https://orcid.org/0000-0003-4731-3541

Marion Prudent
Fabiano Sillo
Francesca DEGAN
Mickael LAMBOEUF
Christian JEUDY
Raffaella Ballestrini

Research Article

Keywords: cereals, wheat, Triticum aestivum L., phosphorus, deep phenotyping, root morphology, acquisition efficiency, use efficiency

Posted Date: November 20th, 2026

DOI: https://doi.org/10.21203/rs.3.rs-11348128/v1

License: This work is licensed under a Creative Commons Attribution 4.0 International License.
Read Full License

Title

Deciphering key root traits involved in phosphorus deficiency tolerance of bread wheat (*Triticum aestivum L.)*

Authors

Christian Jeudy[1], Mickael Lamboeuf[1], Marion Prudent[1], Francesca Degan[2], Raffaella Balestrini[3], Fabiano Sillo[4], Christophe Salon[1*]

Affiliations

[1] Université Bourgogne Europe, Institut Agro Dijon, INRAE, Agroécologie, Dijon, France

[2]ARVALIS, Station Expérimentale de Boigneville, 91270 Boigneville, France.

[3]National Research Council of Italy, Institute of Biosciences and Bioresources (CNR-IBBR), 70126 Bari, Italy.

[4]National Research Council of Italy, Institute for Sustainable Plant Protection (CNR-IPSP), 10135 Torino, Italy.

* Address correspondence to: Christophe Salon; christophe.salon.pons@gmail.com,

ORCHID

M Lamboeuf: 0000-0002-6173-4011

M Prudent: 0000-0003-4696-2558

F Degan: 0000-0002-1782-3228

R Balestrini: 0000-0001-7958-7681

F Sillo: 0000-0002-1218-9985

C Salon: 0000-0003-4731-3541

ABSTRACT

Background and Aims: Crops adapt to phosphorus (P) deficiency primarily by modifying their root system. A high-throughput phenotyping platform was used to identify root traits linked to P-deficiency tolerance in 30 bread-wheat (*Triticum aestivum* L.) genotypes.

Methods: P acquisition efficiency (PAE), P use efficiency (PUE) and phosphorus-related acquisition efficiency (PRAE) were estimated with three indicators. Plants were grown under controlled, low-P conditions on a non-destructive phenotyping platform. After 30 days, shoot biomass was recorded and a deep-root phenotyping pipeline quantified a range of root

morphological traits and their dynamics. Relations between root traits and the three P-efficiency indicators were explored, including a Random-Forest analysis.

Results: The screening distinguished genotypes with contrasting capacities to acquire and/or use P under limitation. Random-Forest analysis showed that PAE and PUE were mainly associated with total root length, exploration area and root density, whereas PRAE exhibited only weak links with the measured morphometric traits.

Conclusion: Combining static root morphometrics with dynamic, non-destructive monitoring allowed the identification of traits characterising the most P-efficient genotypes and clarified whether they relate to acquisition or utilization under low-P conditions.

Key words: cereals, wheat, *Triticum aestivum* L., phosphorus, deep phenotyping, root morphology, acquisition efficiency, use efficiency

INTRODUCTION

Phosphorus (P) is a key nutrient in agricultural systems because of its low mobility in soils and the generally limited ability of crops to acquire it (Roberts and Johnston 2015). In cereals, and especially bread wheat (*Triticum aestivum* L.), P deficiency reduces both grain yield and quality (Dhillon et al. 2017; Yan et al. 2021). Wheat is one of the most widely cultivated cereals worldwide (Dharmateja et al. 2021; Soumya et al. 2022) and has a higher dependence on phosphate fertilizers than many other crops (Heffer 2013). Applying P-containing fertilizers to compensate for low soil P availability is often inefficient, as the apparent recovery of fertilizer P by crops in the year of application is commonly low, around 10–15 % depending on the calculation method. The unrecovered P may accumulate in soil pools of varying availability and, under conditions favoring runoff or erosion, contribute to P transfers to surface waters and eutrophication (Roberts and Johnston 2015). Moreover, phosphorus is a non-renewable resource whose reserves are rapidly declining (Dawson and Hilton 2011). Therefore, developing P-efficient germplasm is essential—and indeed mandatory—for promoting agro-ecological practices under low-P soil conditions (Wang et al. 2010).

Plant adaptation to P scarcity involves two complementary efficiencies: phosphorus acquisition efficiency (PAE), which reflects the plant's capacity to take up P from the soil, and phosphorus use efficiency (PUE), which describes how effectively the acquired P is converted into biomass. Both are shaped by genetic and environmental factors. When confronted with low P availability,

wheat modifies its root system architecture (RSA) and root morphology, and may also adjust root functional traits (Shen et al. 2018; Wang et al. 2021).

Typical morphological adaptations observed in P-efficient genotypes include: increased root density and a higher number of lateral branches (Wang et al. 2019); longer primary and lateral roots and greater root diameter (Dharmateja et al. 2021); enhanced root-hair development (Bates and Lynch 2001); shallower root systems that exploit the P-rich upper soil layers (Jia et al. 2018; Sun et al. 2018).

Functional RSA responses further involve the secretion of various exuded compounds such as protons, organic acids (e.g., citrate, malate), anions and enzymes such as acid phosphatases, which acidify the rhizosphere (Vance et al. 2003; Wen et al. 2019; Yan et al. 2004). Plants also improve local P availability through interactions with phosphate-solubilising microorganisms (Fang et al. 2024; Gahoonia and Nielsen 2004; Marschner et al. 2011; Pang et al. 2018; Robles-Aguilar et al. 2019; Wen et al. 2019; Yang et al. 2012; Zhang et al. 2018) and with arbuscular mycorrhizal fungi that extend the soil volume explored for P acquisition (Zhang et al. 2018).

PUE of the absorbed P requires complex, integrated processes at whole-plant, tissue, cellular and sub-cellular levels, including P transport and metabolism, storage, and remobilisation (Han et al. 2022).

Trade-offs can arise not only between morphological traits (*e.g.*, root biomass, length, hair development, density) that increase the absorptive surface (Da Silva et al. 2016; Nguyen and Stangoulis 2019) but also between morphological and functional traits. For instance, an investment in extensive root architecture may reduce resources available for root exudation, whereas high exudation per unit root (specific exudation activity) can enhance soil P solubilisation (Li et al. 2024) or facilitate recruitment of beneficial microbiota. Assessing which root traits contribute to phosphorus acquisition versus utilisation efficiency remains challenging, especially at high-throughput scale (Lambers et al. 2006).

The present study aimed to:

a. Characterise the growth responses of a panel of wheat genotypes to low-P conditions under controlled conditions using the 4PMI high-throughput phenotyping platform;
b. Identify contrasting genotype adaptation strategies based on phosphorus acquisition and utilisation efficiencies;
c. Investigate relationships between root morphological and physiological traits and the identified adaptation strategies.

MATERIALS AND METHODS

Experimental and technical design:

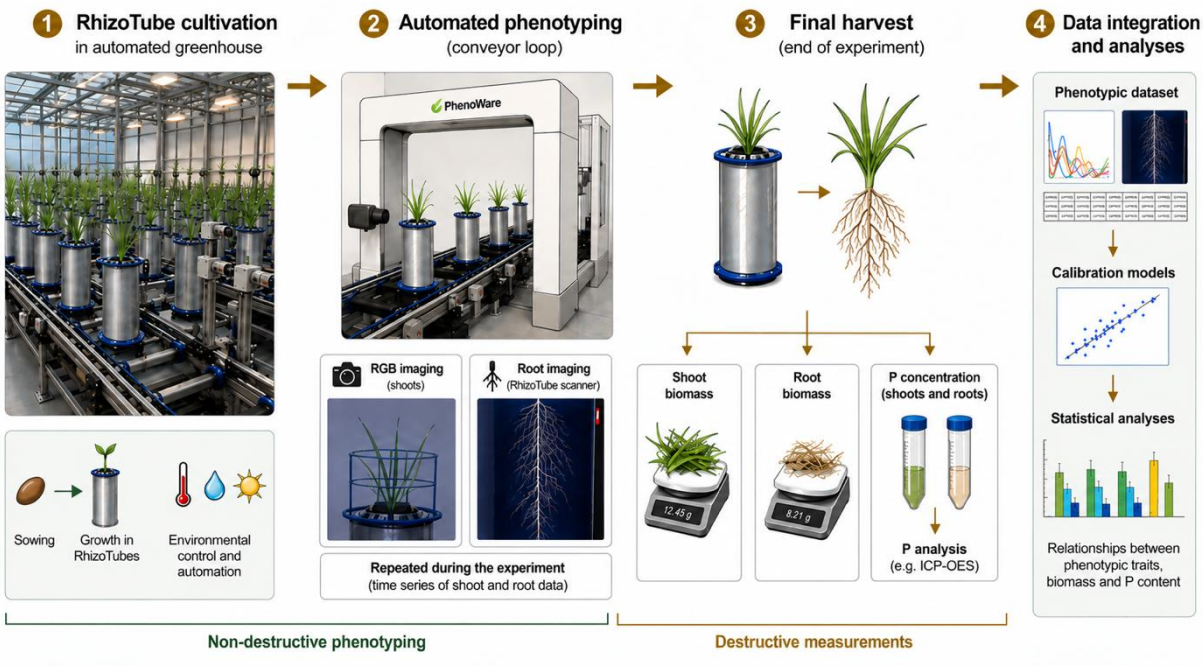


Fig. 1. Comprehensive experimental design and workflow for phenotyping of bread-wheat for phosphorus deficiency using high throughput root phenotyping.

Plant material and growth conditions

Thirty bread-wheat (*Triticum aestivum L.*) genotypes were examined (Table 1). Twenty-six of them had previously been characterised for agronomic traits on two phenotyping platforms (Sillo et al. 2025); four additional CIMMYT spring lines were added to broaden the genetic diversity.

Table 1. List of the breadwheat genotypes. Among the evaluated genotypes, three were developed by RAGT Seeds Ltd. (UK) and nine by the International Maize and Wheat Improvement Center (CIMMYT, Mexico).

Genotype	Seed company
Advisor	Limagrain Europe
Alessio	Lemaire Deffontaines
Annecy	Lemaire Deffontaines
Armada	Limagrain Europe
Bagou	Saaten Union
Calixo	Secobra
Cimmyt 4	CIMMYT

Cimmyt 10	CIMMYT
Cimmyt 11	CIMMYT
Cimmyt 12	CIMMYT
Cimmyt 13	CIMMYT
Cimmyt 14	CIMMYT
Cimmyt 15	CIMMYT
Cimmyt 20	CIMMYT
Cimmyt 22	CIMMYT
Complice	Florimond Desprez
Crusoe	LG
Donator	Unisigma
Foxyl	KWS Momont
Gedser	Sem Partners
Hereward	Florimond Desprez
Hyking	Saaten Union
Ionesco	Secobra
Johnson	Saaten Union
Pibrac	Syngenta
RGT Lexio	RAGT
RGT Libravo	RAGT
Robigus	KWS Momont
Rubisko	RAGT
Soissons	Florimond Desprez

Plants were cultivated in the 4PMI high-throughput phenotyping platform (Dijon, France) using RhizoTubes (Jeudy et al. 2016). Each RhizoTube was filled with a sand: perlite mixture (1 : 3 v/v). The greenhouse climate was set at 23.3 °C (day) / 19.3 °C (night), 65 % relative humidity, and a 16 h photoperiod supplemented with 400 W HPS lamps (OSRAM) to obtain an average photosynthetic photon flux density of 355 µmol m^{-2} s^{-1}.

Seeds were surface-sterilised, imbibed in petri dishes at 20 °C for 12 h, then vernalised at 4 °C for 24 h in a Fitoclima S600 germinator (Aralab, Portugal). One seed was transplanted per RhizoTube. Six biological replicates were grown per genotype and per phosphorus level, giving 12 tubes per genotype (total = 360 tubes).

Phosphorus treatments

This paper and its results focus on plants cultivated under low P availability, for which deep phenotyping analyses were performed, rather than on plants grown under optimal P availability as in (Sillo et al. 2025).

Plants were irrigated with a modified Hoagland solution containing 0.0032 mM $NH_4H_2PO_4$ (≈ 1.73 kg ha^{-1}), which represents low-P availability compared with the optimal concentration used in (Sillo et al. 2025). The full nutrient composition was: 3 mM KNO_3, 2 mM $CaCl_2$, 2 mM $MgSO_4 \cdot 7H_2O$, 9.14 µM $MnCl_2 \cdot 4H_2O$, 0.76 µM $ZnSO_4 \cdot 7H_2O$, 0.32 µM $CuSO_4 \cdot 5H_2O$, 0.49 µM $NaMoO_4 \cdot 2H_2O$, 52 µM KFe-EDTA, 46.2µM H3BO3. Solution pH ≈ 6. Prior to transplantation, the RhizoTube substrate was fully saturated with the solution.

Substrate moisture was maintained at ~95 % of its water-holding capacity (≈ 45 % volumetric water content) by three daily irrigations. Each irrigation delivered 25–75 mL per RhizoTube, adjusted according to gravimetric water loss.

Root imaging and image analysis

RhizoTubes were imaged several times per week on the 4PMI RhizoCab HT phenotyping booths (Jeudy et al. 2016). Fourteen phenotyping time-points were collected, yielding 35 760 aerial images and 2 520 root images (13 aerial views + 1 root view per plant per time-point). Image processing comprised two steps: 1) Segmentation – A custom U-Net convolutional neural network performed pixel-wise semantic segmentation to separate root pixels from background. This approach differs from RootNav 2.0 (Yasrab et al. 2019), which is oriented toward architectural tracing. The resulting binary mask was cleaned by retaining the largest continuous white region, thereby eliminating noise and false detections. 2) Trait extraction – Using OpenCV and scikit-image libraries (Bradski 2000; van der Walt et al. 2014), a suite of root morphological descriptors (Fig. 2) was computed, including projected root area, convex hull, root density, centroid coordinates, total root length, mean diameter, etc.

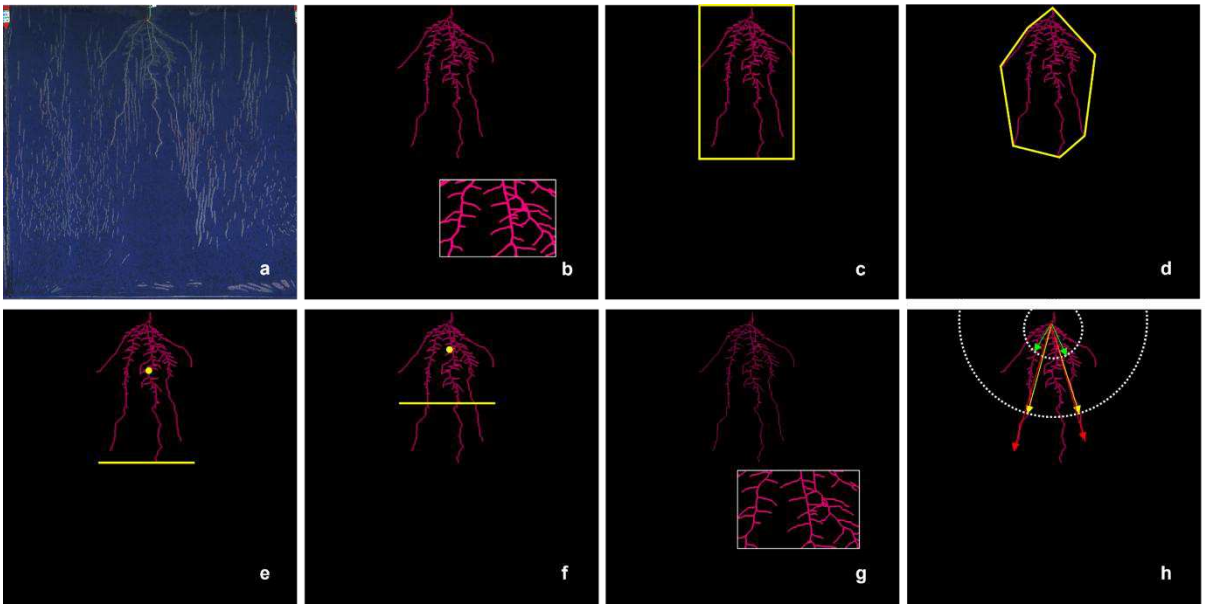


Fig. 2. Root traits extracted from image analysis. Traits were derived from the original root image (**a**). Dynamic traits measured at each of the 14 phenotyping time points included root projected area (RPA, **b**), root bounding box dimensions (height, RBY, and width, RBX; **c**), root convex hull area (RCHA; **d**), and the root center of mass computed along the horizontal (RGCX) and vertical (RGCY) axes (yellow dot). (**e**) Full root system considered (100% of plant height). (**f**) Analysis restricted to the upper 80% of the root system, measured from the top of the image. The yellow horizontal line indicates the lower boundary of the region considered in each case. Total root length obtained using skeletonization of the segmented image (TRL; **g**). Insets shown in panels B and G correspond to zoomed regions of the analysed images. Single time-point traits included root angles (**h**) measured at the intersection with a 60 mm circle (green arrow; SA_60_04), a 250 mm circle (yellow arrow; SA_250_04), and at the root tip (red arrow; ST_60_04), all centred on the seed. Note that the leftmost and rightmost roots were not considered, as they emerged later than the three primary seminal roots.

Trait classification

The 19 measured traits were divided into two groups (Table 2): one-time traits (8): assessed only at a single time-point and dynamic traits (11): measured at every phenotyping time-point, allowing the fitting of growth curves (see Section 5).

Table 2. Shoot and root traits assessed in the study. The "one-time point trait" correspond to trait measured at one unique time during the plant growth while the "dynamic traits" were measured at each phenotyping date. Traits are listed with their acronym and associated formula when appropriate, and broad-sense heritability estimates (H^2).

1

One point traits	Acronym	Formula	Unit	H^2
Sem_Angle_60_DAS04	SA_60_04	At Day 4 angle between left and right seminal at intersection of a 60 mm seed centred cercle	degree	0,73
Sem_Tip_DAS04	ST_04	At Day 4 angle between left and right seminals at the root tip	degree	0,6
Sem_Angle_250_DAS16	SA_250_16	At Day 16 angle between left and right seminal at intersection of a 60 mm seed centred cercle	degree	0,59
Sem_Tip_DAS16	ST_16	At Day 16 angle between left and right seminals at the root tip	degree	0,63
Plant biomass	PB	Dry biomass of plants = RB + SB	g	0.64
Root biomass	RB	Dry biomass of the root system	g	0.75
Shoot biomass	SB	Dry biomass of shoots	g	0.65
Shoot root ratio	SRR	Ratio of shoot over root biomass = SB/RB		0.93
Dynamic traits	**Acronym**	**Formula**		
Root_Convex_Hull_Area	RCHA	Prospection area of roots	mm^2	0,64
Root_Projected_Area	RPA	2D root projected area	mm^2	0,52
Root_BoundingBox_X	RBX	Width of the root bounding box	mm	0,48
Root_BoundingBox_Y	RBY	Height of the root bounding box	mm	0,41
Root_Gravity_Center_X	RGCX	Position along the height axis of the mass center	mm	0,05
Root_Gravity_Center_Y	RGCY	Position along the width axis of the mass center	mm	0,73
Root_Gravity_Center_X_80	RGCX80	Gravity center position along the height axis using only 80% of the root along the width axis	mm	0,10
Root_Gravity_Center_Y_80	RGCY80	Position of the gravity center using only 80% of the plant root along the width axis	mm	0,74
Mean_Root_Diameter	MRD	Averaged diameter of the whole root plant computed from local diameters	mm	0,46
Total_Root_Length	TRL	Sum of all root lengths	mm	0,51
Root_Density	RD	Ratio of the 2D root area to the root convex hull area = RPA/RCHA		0,71

2

2.1.1 *One-time root-angle measurements*

Root angles were obtained with a dedicated software developed at the 4PMI platform (Maslard et al. 2026).

At the 4th days after sowing (DAS4), two angles were recorded:

- Sem_Angle_60_04 (SA_60_04) – angle between left and right seminal roots at the intersection with a 6 cm-diameter circle centred on the seed;
- Sem_Tip_DAS04 (ST_04) – angle between the same roots at the root tip.

At DAS16, the analogous measurements were Sem_Angle_250_DAS16 (SA_250_16) (intersection with a 25 cm-diameter circle) and Sem_Tip_DAS16 (ST_16).

2.1.2 *Dynamic trait modelling*

For each dynamic trait, values across the fourteen time-points were fitted with a smooth curve using the statgenHTP R package (Millet et al. 2021). From each curve four parameters were extracted:

- X_min_value : minimum observed value,
- X_max_value : maximum observed value,
- X_max_deriv : maximal growth rate (first derivative),
- X_time_max_deriv : time at which the maximal growth rate occurs.

The first derivative was obtained from the fitted spline using the 'deriv()' function in the *statgenHTP* package. These parameters capture the magnitude, speed, and timing of trait development, facilitating biological interpretation (e.g., a high X_max_deriv for root convex-hull area indicates rapid root-system expansion).

Harvest measurements, phosphorus analysis and Phosphorus efficiency indicators

At the end of the experiment, shoots and roots were harvested, oven-dried at 60 °C for 72 h and weighed to obtain shoot biomass (SB) and root biomass (RB). The shoot-to-root ratio (SRR) was calculated as SB / RB.

Phosphorus content in dry tissue was quantified by high-resolution inductively coupled plasma mass spectrometry (HR-ICP-MS, Thermo Scientific Element 2) after microwave acid digestion (Multiwave ECO, Anton Paar) with HNO_3 and H_2O_2. Internal standards (Ga = 5 mg L^{-1}, Rh = 1 mg L^{-1}) were added, samples were diluted to 2 % HNO_3, filtered (0.45 µm PTFE) and expressed in ppm.

Three P-efficiency indices were calculated at harvest following (Sillo et al. 2025), (Table 3): Phosphorus Acquisition Efficiency (PAE) is the proportion of supplied P that was taken up by the plant. Whole plant Phosphorus Utilisation Efficiency (PUE) is the amount of total plant

dry-biomass produced *per* unit of P absorbed. Phosphorus Root Acquisition Efficiency (PRAE) is the quantity of P taken up *per* unit of root biomass.

Table 3. Definition, formulas, units, and references of the phosphorus efficiency indicators used in this study to characterise phosphorus acquisition and utilisation performances of wheat genotypes under low phosphorus availability.

Indicator name	Acronym	Formula	Unit	Reference
Phosphorous Acquisition Efficiency	PAE	PAE = (P uptake/P applied) *100 = P per plant/ P per substrate * 100		Han *et al.* 2022
Phosphorus Utilisation Efficiency	PUE	PUE = Plant dry weight / P concentration in plant * Plant dry weight	g DM g^{-1} P	Syers *et al.* 2008
Phosphorus Root Acquisition Efficiency	PRAE	PRAE = P uptake / Roots_Biomass	g P g^{-1} DM	Sillo *et al.* 2025

Statistical analysis

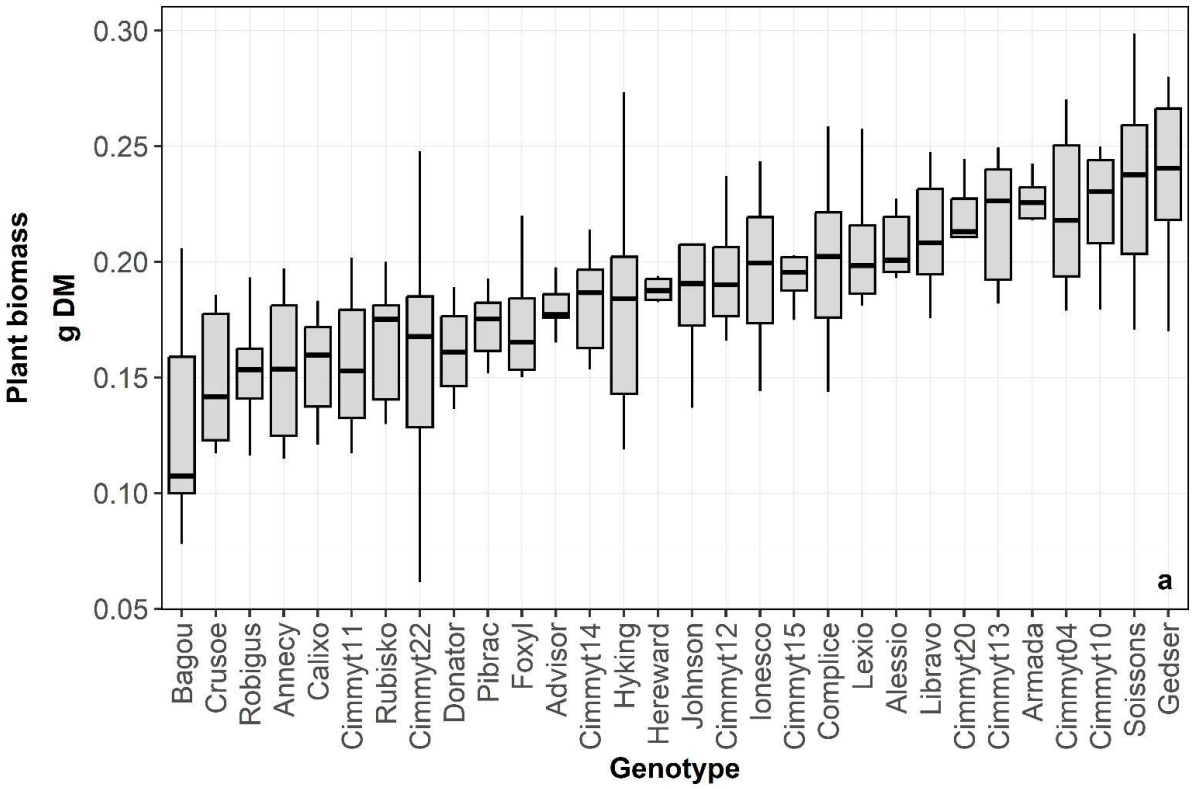
Analyses were performed in R software (R Core Team 2024). Outlier detection and environmental correction (greenhouse position) were carried out with the **StatgenHTP** and **Spats** packages. Missing values were imputed using **missMDA**. Heritability of each trait was estimated, and dynamic curves were fitted as described in Section 5. Principal component analysis (PCA) employed **FactoMineR**. One-way ANOVA compared P-efficiency indicators among genotypes. Random-forest models were built with the **randomForest** package (Liaw and Wiener 2002) to identify traits most predictive of P efficiency indicators.

RESULTS

Genotypic differences in plant biomass and shoot-to-root ratio

As reported by (Sillo et al. 2025), the 30 wheat genotypes displayed significant variation in shoot and root biomass under both limiting and non-limiting phosphorus (P) conditions. In the present experiment the very low P availability reduced overall growth compared with the P + treatment of (Sillo et al. 2025), but it also revealed strong genotype-dependent responses (Fig. 3).

A highly significant genotype effect was detected for total plant biomass (ANOVA, $P < 0.001$). For example, the genotype Bagou produced up to 84 % less biomass than the most productive genotype Gedser at the end of the trial (Fig. 3).



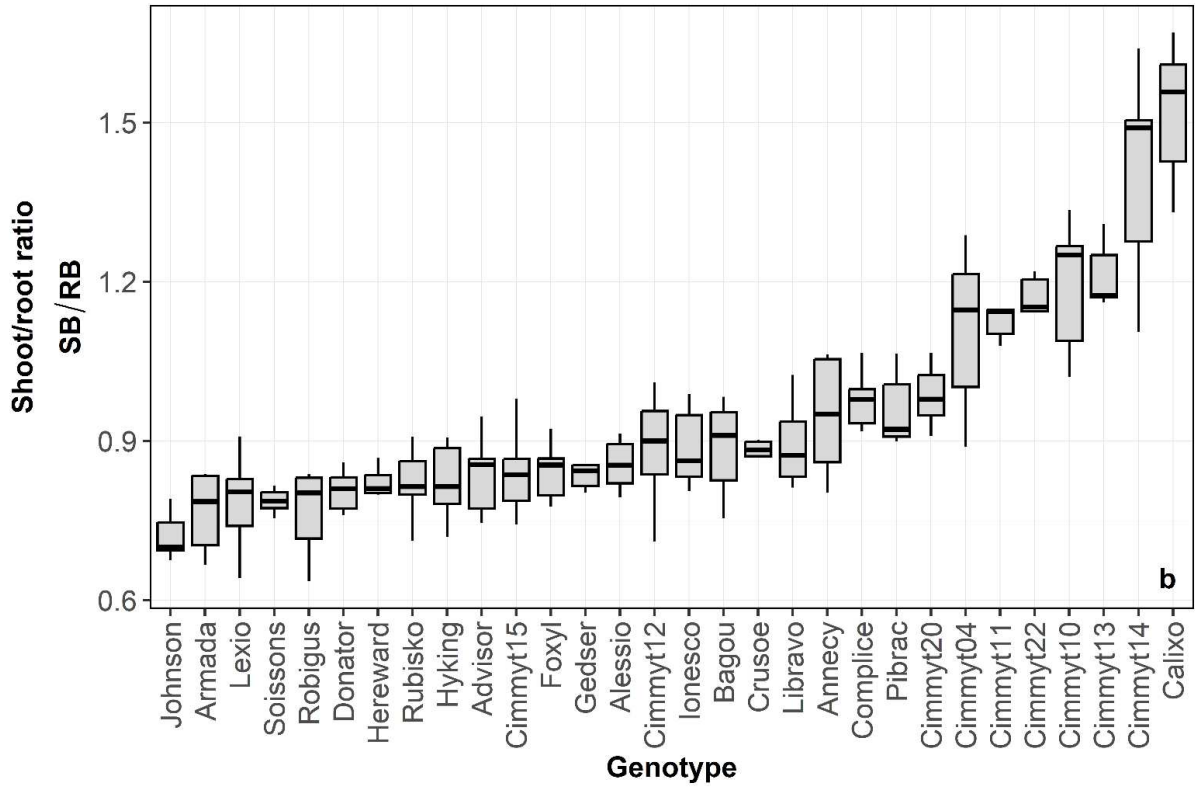


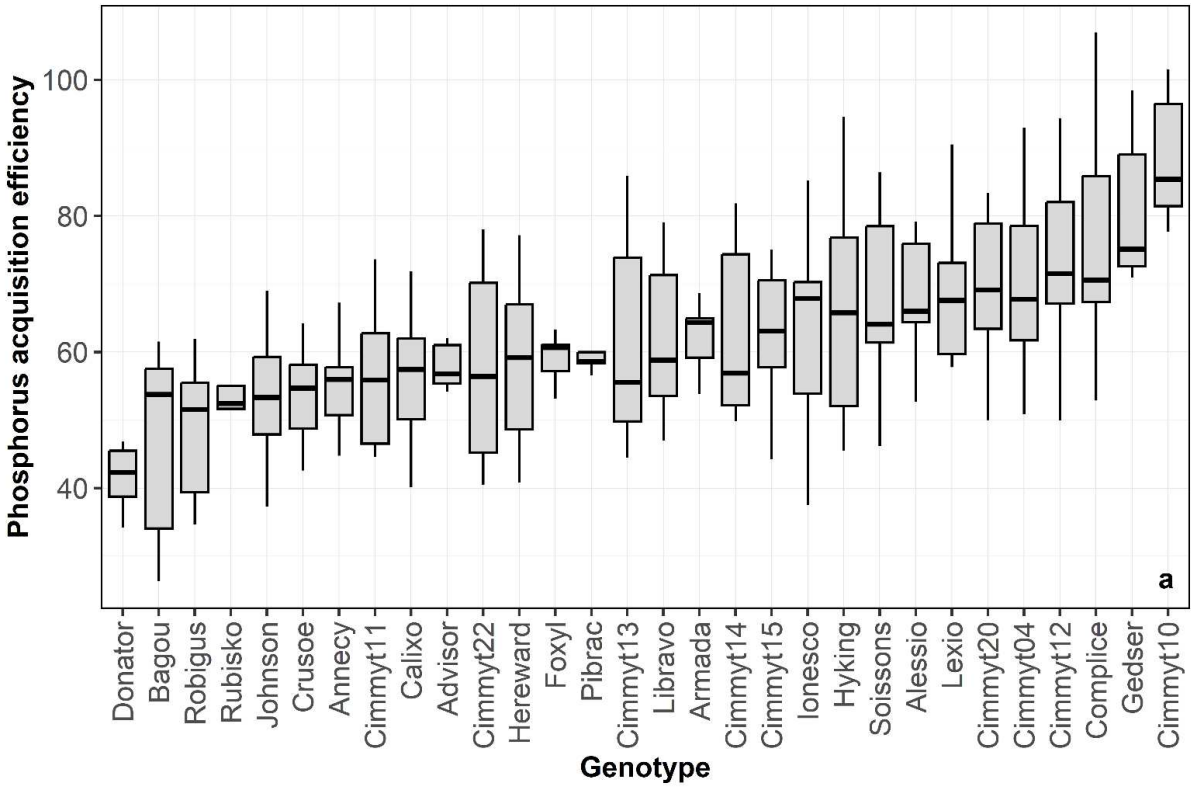
Fig. 3. Variation in plant biomass (**a**) and shoot/root ratio (**b**) among wheat genotypes grown under low phosphorus availability. Boxplots represent the distribution of values measured for each genotype. (6 biological replicates).

Genotype also significantly affected SRR (ANOVA, $P < 0.001$). CIMMYT lines generally exhibited higher SRR values, indicating a stronger allocation of assimilates to the shoot relative to the root. No simple relationship was found between total biomass and SRR ($r^2 = 0.003$); genotypes with similar SRR could differ markedly in absolute biomass (*e.g.*, Gedser *vs*. Bagou).

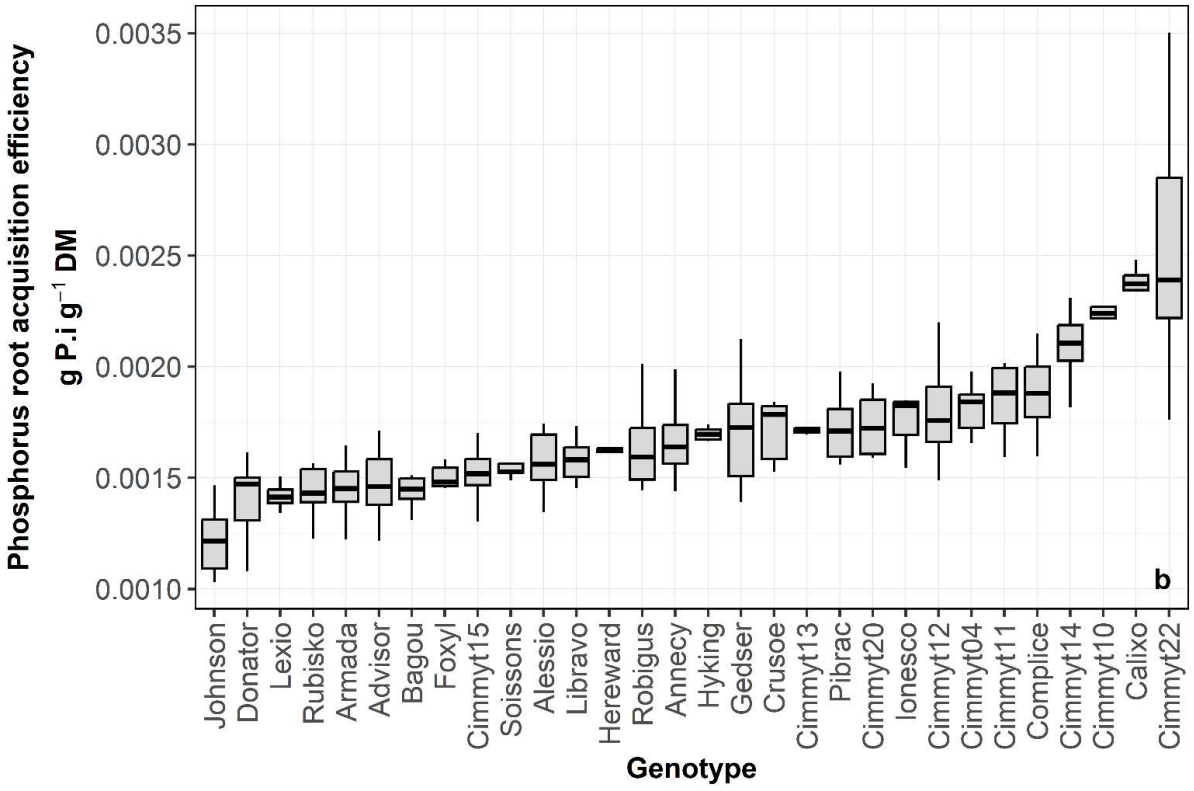
These results confirm that, under severe P limitation, genotypic diversity translates into contrasting growth strategies and biomass partitioning.

Genotypic differences in phosphorus-efficiency indicators

To explore the underlying strategies, the three efficiency indicators—phosphorus acquisition efficiency (PAE), root acquisition efficiency (PRAE) and phosphorus use efficiency (PUE)—were calculated for each genotype (Fig. 4).


Phosphorus acquisition efficiency
100
80
60
40
a
Donator
Bagou
Robigus
Rubisko
Johnson
Crusoe
Annecy
Cimmyt11
Calixo
Advisor
Cimmyt22
Hereward
Foxyl
Pibrac
Cimmyt13
Libravo
Armada
Cimmyt14
Cimmyt15
Ionesco
Hyking
Soissons
Alessio
Lexio
Cimmyt20
Cimmyt04
Cimmyt12
Complice
Gedser
Cimmyt10
Genotype

1


Phosphorus root acquisition efficiency
g P.i g^{-1} DM
0.0035
0.0030
0.0025
0.0020
0.0015
0.0010
b
Johnson
Donator
Lexio
Rubisko
Armada
Advisor
Bagou
Foxyl
Cimmyt15
Soissons
Alessio
Libravo
Hereward
Robigus
Annecy
Hyking
Gedser
Crusoe
Cimmyt13
Pibrac
Cimmyt20
Ionesco
Cimmyt12
Cimmyt04
Cimmyt11
Complice
Cimmyt14
Cimmyt10
Calixo
Cimmyt22
Genotype

2

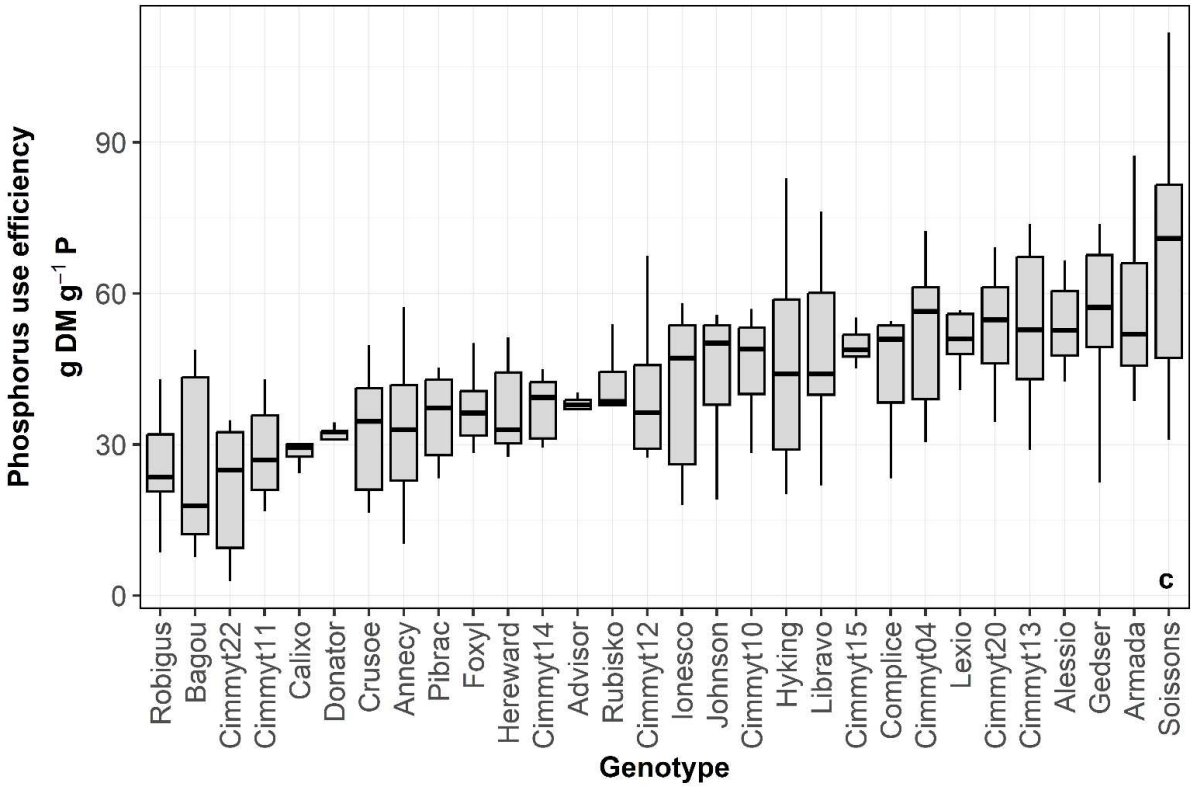


Fig. 4. Genotype ranking on their Phosphorus Acquisition Efficiency – PAE - (**a**), Phosphorus Root Acquisition Efficiency -PRAE - g Pi g^{-1} DM - (**b**), Phosphorus Utilization Efficiency – PUE - g DM g^{-1} Pi (**c**).

- *High PRAE, low PUE.* CIMMYT22 and Calixo displayed the highest PRAE (*i.e.*, the most P captured per unit root mass) but the lowest PUE, indicating that the acquired P was not efficiently converted into biomass. Consequently, these genotypes ranked among the lowest in final biomass (Fig. 3).
- *Low PRAE, high PUE.* Armada and Lexio showed the opposite pattern: modest PRAE but relatively high PUE, suggesting that a lower *per*-unit-root P acquisition is compensated by a larger root system and more efficient P utilisation. Both genotypes also had the lowest SRR, reflecting a greater investment in root biomass.
- *Balanced performance.* – CIMMYT10 combined high PAE and PRAE with an intermediate PUE, whereas Bagou performed poorly across all three indicators (low PAE, low PRAE, low PUE), which explains its minimal biomass accumulation.

These contrasting profiles illustrate that a genotype can achieve comparable P acquisition through either (i) high efficiency per unit root (high PRAE) or (ii) greater root biomass (low PRAE but low SRR), the latter being associated here with higher PUE.

Principal component analysis (PCA) of efficiency traits

A PCA was carried out to visualise the relationships among genotypes and the three efficiency indicators (Fig. 5). Component 1 captured the positive covariance between PAE and PUE, while PRAE loaded negatively, confirming that genotypes with high acquisition efficiency also tended to use the acquired P efficiently, whereas high root-acquisition efficiency (PRAE) was largely independent of the other two traits.

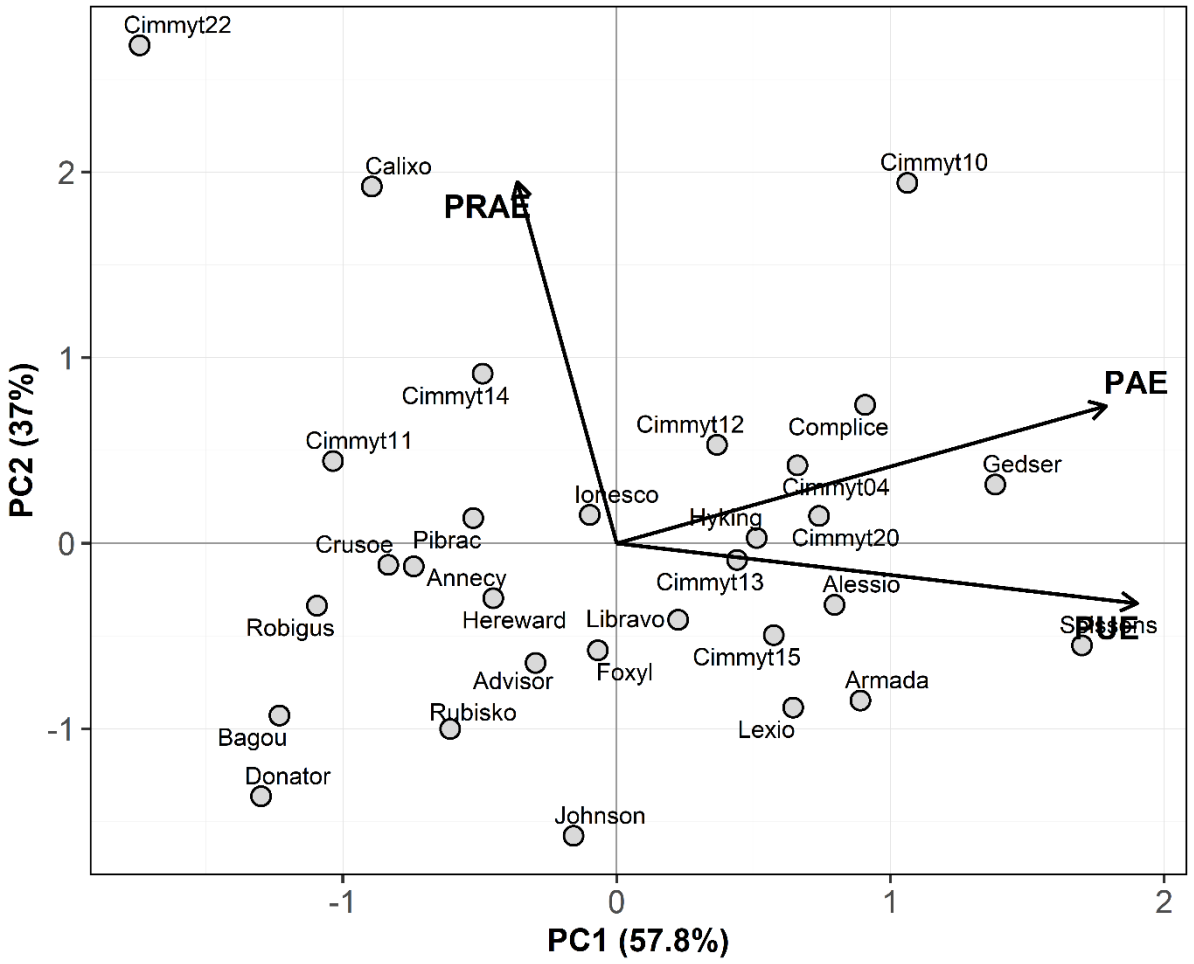


Fig. 5. Principal component analysis (PCA) based on phosphorus efficiency indicators under low phosphorus availability. Positioning of the various genotype, principal component analysis realized on acquisition and use efficiency indicators: Phosphorous Acquisition Efficiency (**PAE**), Phosphorus Utilisation Efficiency (**PUE**), Phosphorus Root Acquisition Efficiency (**PRAE**). Point displayed are the average of a given genotype. The PCA was performed using phosphorus acquisition efficiency (PAE), phosphorus utilisation efficiency (PUE), and physiological phosphorus acquisition efficiency (PRAE). Each point represents the

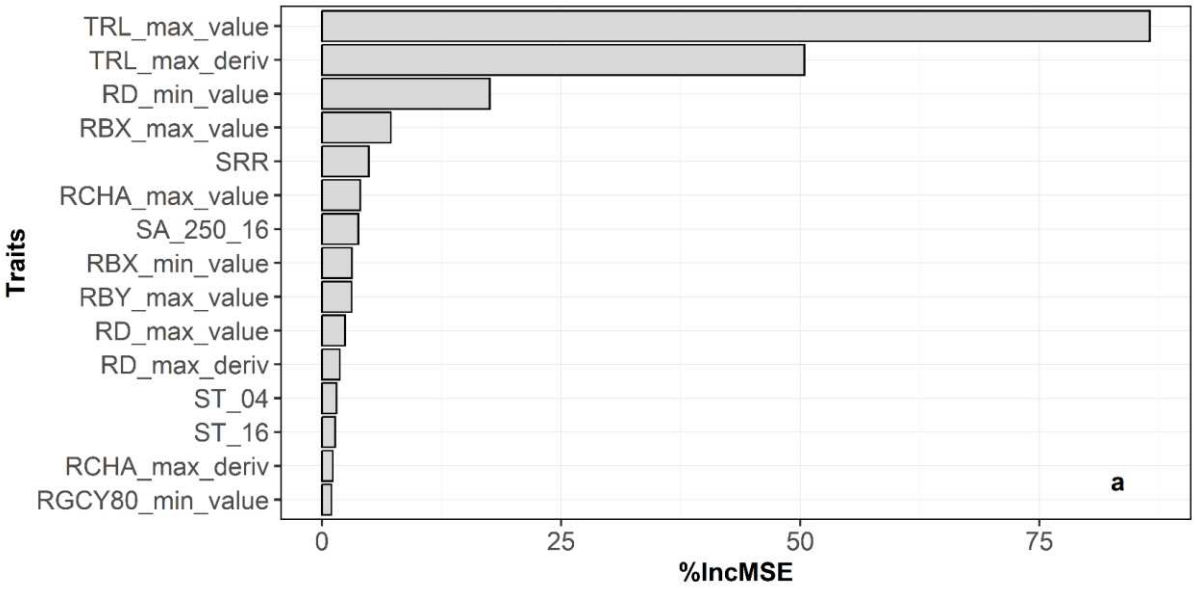
mean position of a genotype calculated from individual plant coordinates in the PCA space. Arrows indicate the contribution and direction of the phosphorus efficiency indicators to the principal components. PC1 and PC2 explained 57.8% and 37% of the total variance, respectively.

Gedser and Soisson clustered in the quadrant of high PAE / high PUE, whereas Bagou and Donator were positioned towards low values of both. The distribution, however, remained diffuse; no clearly defined genotype groups emerged, indicating that the adaptive strategies are spread along a continuum rather than forming discrete clusters.

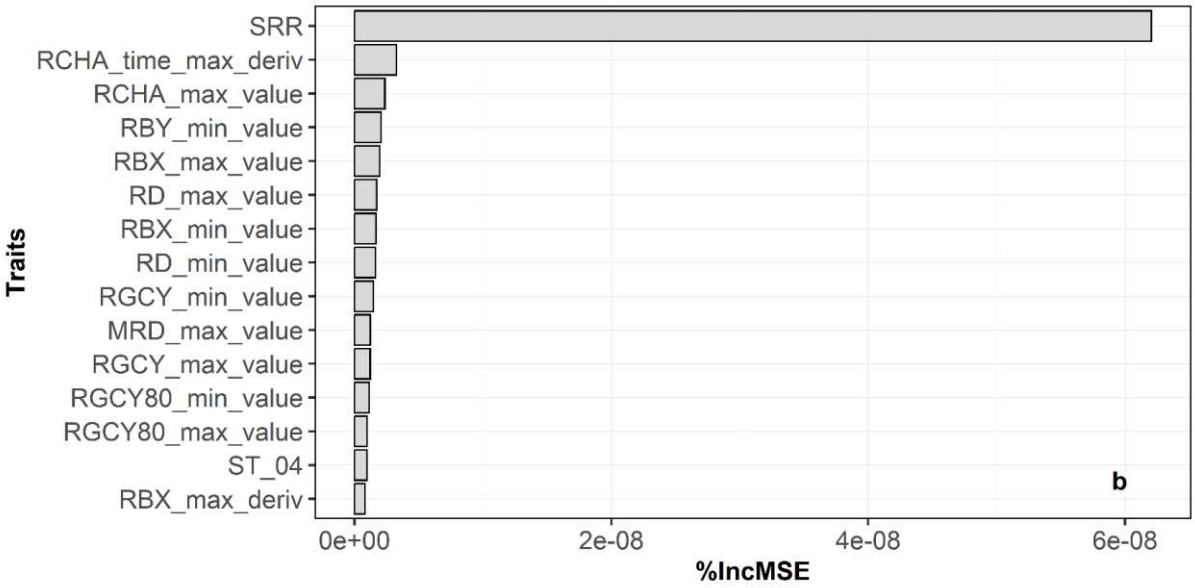
These results highlight that wheat genotypes adopt different combinations of root acquisition and phosphorus utilisation to cope with severe P limitation, providing a basis for selecting traits that could be combined in future ideotypes.

Random Forest analysis of phosphorus-efficiency indicators and deep-phenotyping traits

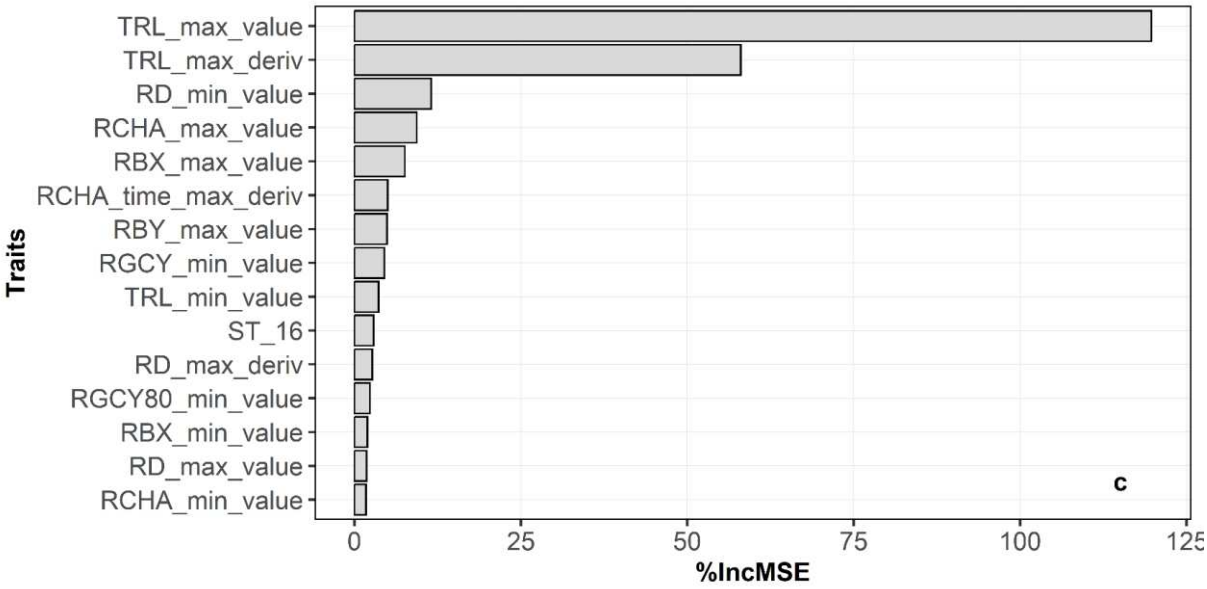
After the genotypes with contrasting phosphorus-acquisition efficiency (PAE and PRAE) and phosphorus-use efficiency (PUE) had been identified (Fig. 4), we explored how the phenotypic traits measured by the 4PMI platform related to these efficiencies (Fig. 6).


TRL_max_value
TRL_max_deriv
RD_min_value
RBX_max_value
SRR
RCHA_max_value
SA_250_16
RBX_min_value
RBY_max_value
RD_max_value
RD_max_deriv
ST_04
ST_16
RCHA_max_deriv
RGCY80_min_value
Traits
0
25
50
75
%IncMSE
a

1


SRR
RCHA_time_max_deriv
RCHA_max_value
RBY_min_value
RBX_max_value
RD_max_value
RBX_min_value
RD_min_value
RGCY_min_value
MRD_max_value
RGCY_max_value
RGCY80_min_value
RGCY80_max_value
ST_04
RBX_max_deriv
Traits
0e+00
2e-08
4e-08
6e-08
%IncMSE
b

2


TRL_max_value
TRL_max_deriv
RD_min_value
RCHA_max_value
RBX_max_value
RCHA_time_max_deriv
RBY_max_value
RGCY_min_value
TRL_min_value
ST_16
RD_max_deriv
RGCY80_min_value
RBX_min_value
RD_max_value
RCHA_min_value
Traits
0
25
50
75
100
125
%IncMSE
c

3

Fig. 6. Random Forest analysis identifying the most important phenotypic traits associated with phosphorus efficiency indicators under low phosphorus availability. Random Forest models were fitted using phenotypic traits as explanatory variables and phosphorus efficiency indicators as response variables: phosphorus acquisition efficiency (PAE, **a**), physiological root acquisition efficiency (PRAE, **b**), and phosphorus use efficiency (PUE, **c**). Barplots represent the 15 most important explanatory traits ranked according to the increase in mean squared error (%IncMSE) following variable permutation. Higher %IncMSE values indicate a greater contribution of the trait to model prediction accuracy.

Relationships with phosphorus-acquisition efficiency (PAE) (Fig. 6A)

The five traits that contributed the most to the Random Forest model for PAE (each accounting for ≥ 8 % of the maximal %IncMSE) were:

- TRL_max_value (maximum total root length) which is a Proxy for overall root exploration capacity,
- TRL_max_deriv (maximum derivative of total root length) reflecting the speed of root elongation during the experiment,
- RD_min_value (minimum root density) which captures a specific root-exploration strategy that is reached after ≈ 15 days and then stabilises,
- RBX_max_value (maximum root width) describing lateral-root expansion and therefore contributes to soil probing,
- SRR (shoot-to-root biomass ratio) Indicates the plant's carbon-allocation strategy.

Together, these variables explain a large fraction of the variability in PAE, emphasizing the importance of both the extent of root system exploration and the dynamics of root growth.

Relationships with phosphorus-root acquisition efficiency (PRAE) - (Fig. 6B)

The Random Forest model yielded very low %IncMSE values for PRAE, indicating that the morphometric traits recorded in this study do not explain the observed variation in PRAE. This suggests that either other morphological factors such as root hairs, or non-morphological factors (*e.g.*, root exudation, mycorrhizal colonisation), may drive PRAE under low-P conditions.

Relationships with phosphorus-use efficiency (PUE) - (Fig. 6C)

Traits identified for PUE closely overlapped those for PAE, which is consistent with the strong positive correlation between the two indicators (Fig. 5). The most important variables were, in addition to TRL_max_value and TRL_max_deriv already mentioned for PAE:

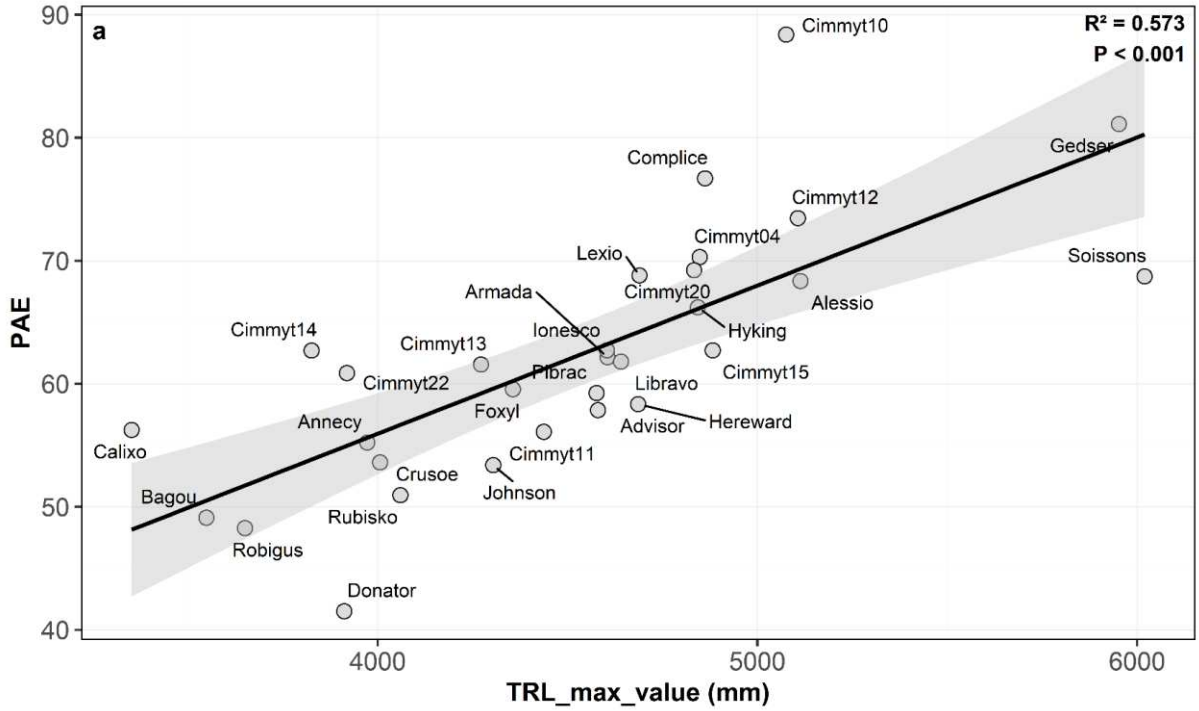
- RCHA_max_value (maximum convex-hull area, another proxy for exploration space),
- RBX_max_value (maximum root width),
- RD_min_value (minimum root density).

These results reinforce the notion that efficient use of acquired phosphorus is linked to a well-developed, dynamically expanding root system.

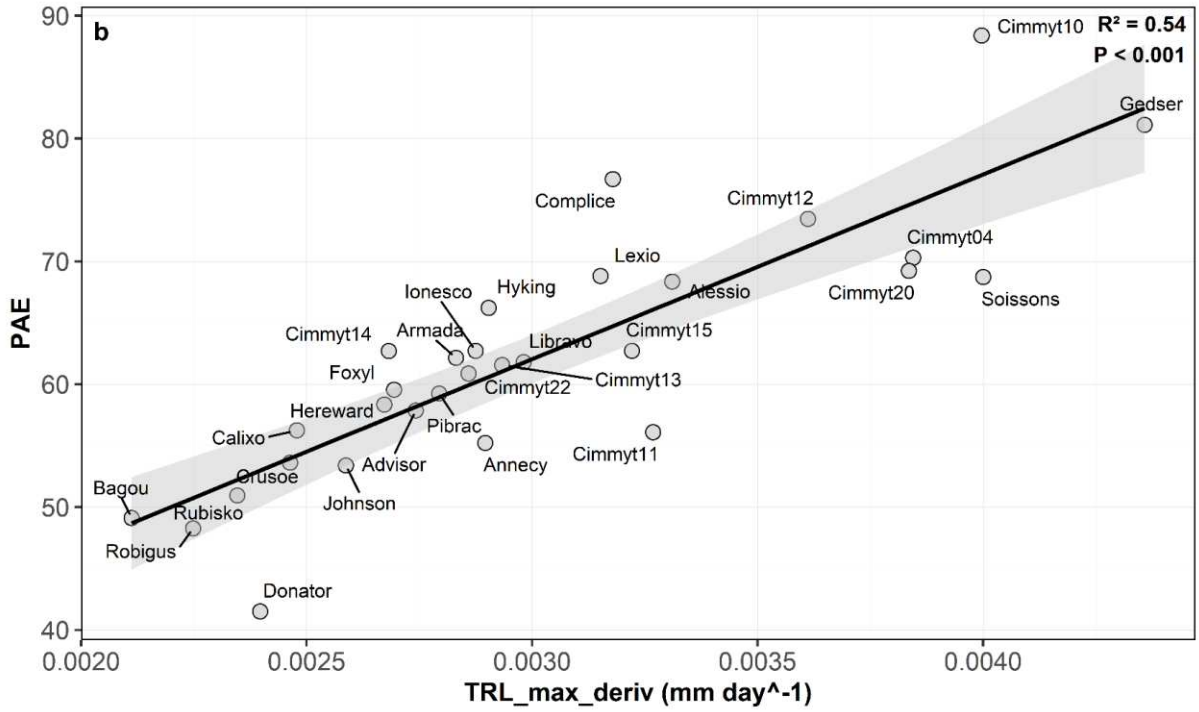
Illustrative relationships

Four representative traits were plotted against PAE (chosen because PAE and PUE are positively correlated) to visualise the trends identified by the Random Forest analysis:

TRL_max_value and TRL_max_deriv displayed a strong linear increase with PAE with longer roots and higher elongation rates detected for Gedser and the shortest for Bagou **(**Fig. 7A and 7B**)**. RD_min_value which represents a more open root architecture is slightly associated with greater PAE **(**Fig. 7C**)**. SRR which displayed no significant linear trend, yet retained by the Random Forest model, hinting at a non-linear or interaction effect of carbon allocation on P acquisition **(**Fig. 7D**)**. Other traits such as RCHA_max_value or RBX_max_value were omitted because they convey information redundant with TRL_max_value (all describe root exploration capacity).


a
R² = 0.573
P < 0.001
PAE
TRL_max_value (mm)
Cimmyt10
Gedser
Complice
Cimmyt12
Cimmyt04
Lexio
Soissons
Armada
Cimmyt20
Alessio
Cimmyt14
Ionesco
Hyking
Cimmyt13
Cimmyt15
Cimmyt22
Pibrac
Libravo
Foxyl
Annecy
Advisor
Hereward
Calixo
Cimmyt11
Crusoe
Johnson
Bagou
Rubisko
Robigus
Donator

1


b
Cimmyt10 R² = 0.54
P < 0.001
PAE
TRL_max_deriv (mm day^-1)
Gedser
Complice
Cimmyt12
Cimmyt04
Lexio
Ionesco
Hyking
Alessio
Cimmyt20
Soissons
Cimmyt14
Armada
Libravo
Cimmyt15
Foxyl
Cimmyt22
Cimmyt13
Hereward
Calixo
Pibrac
Cimmyt11
Advisor
Annecy
Crusoe
Bagou
Johnson
Rubisko
Robigus
Donator

2

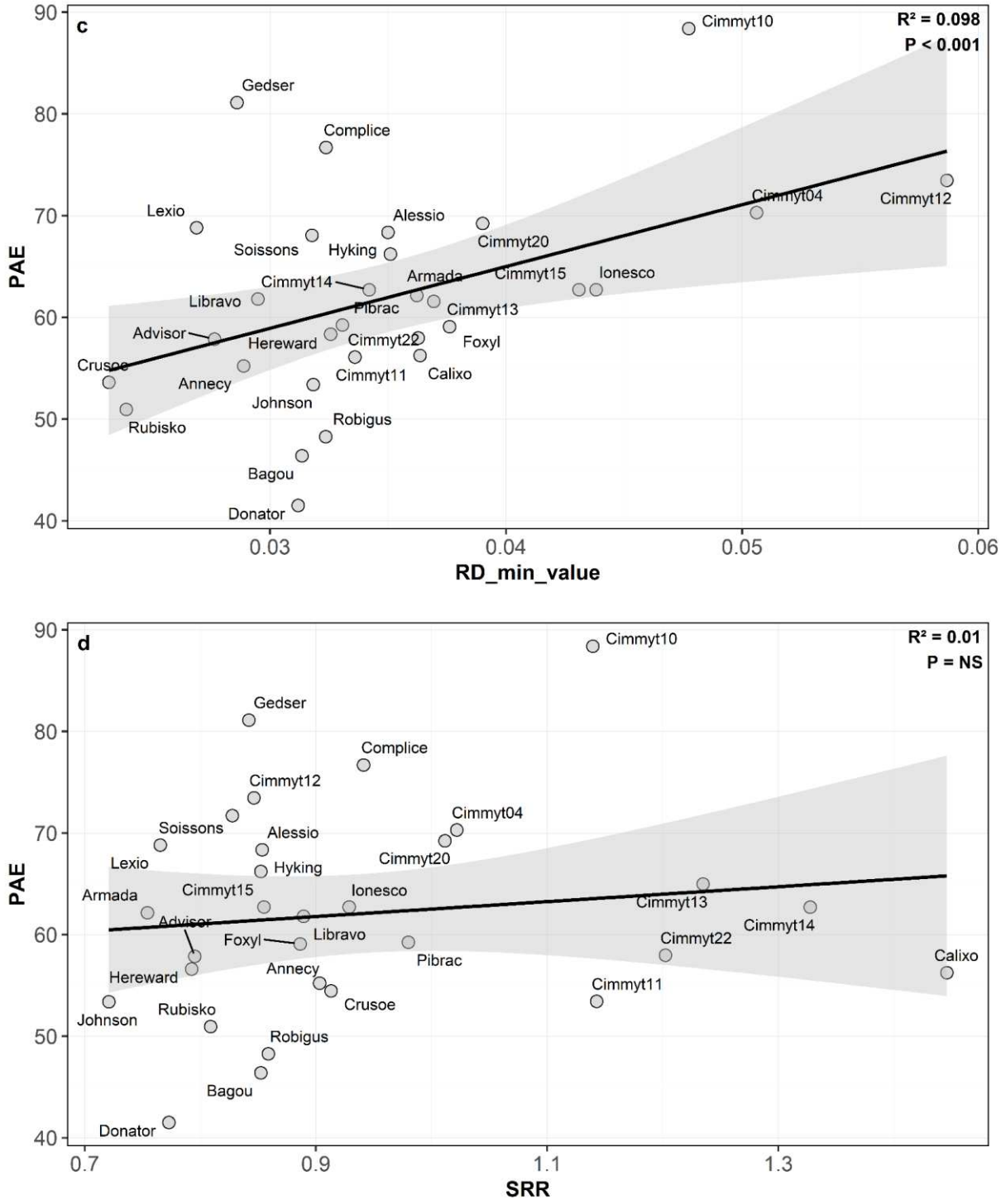


Figure 7. Relationships between phosphorus acquisition efficiency (PAE) and representative root traits identified by Random Forest analysis: (**a**) TRL_max_value, (**b**) TRL_max_deriv, (**c**) RD_min_value and (**d**) SRR. Each point is a mean value of one genotype. Solid lines represent linear regressions, shaded areas are the associated 95% confidence intervals. The reported R^2 and P-values were calculated using all individual observations.

Heritability of key traits

Broad-sense heritability (H^2) was estimated for the traits most strongly linked to PAE and PUE (Table 2). All displayed relatively high H^2 values (> 0.46), indicating substantial genetic control: These heritable traits constitute promising selection targets for breeding programmes aimed at improving phosphorus acquisition and utilisation under low-P conditions.

DISCUSSION

Root architecture as a key factor in phosphorus-deficiency tolerance

Root-architectural traits are central targets for improving both phosphorus (P) acquisition and its subsequent translocation to the shoot. Under P-deficiency wheat typically responds by: increasing lateral-root number and root-hair density (Lynch 2007), reducing primary-root length (Niu et al. 2013), adopting shallower root angles (Lynch 2007).

These morphological adjustments enhance soil-exploration capacity but incur carbon costs that can create trade-offs (*e.g.*, thinner roots versus longer hairs). Functional traits such as root exudation, rhizosphere acidification and symbiotic interactions with mycorrhizal fungi also improve P availability, yet their inheritance is harder to dissect because they involve complex biochemical pathways. Historically, most studies have focused on traits linked to phosphorus-acquisition efficiency (PAE), whereas phosphorus-use efficiency (PUE) – which depends on P transport, storage, remobilisation and the downstream metabolic processes (*e.g.*, energy production, nucleic-acid synthesis) – remains less well characterised. Measuring these functional traits at high-throughput and in a dynamic fashion is considerably more challenging than measuring morphological traits with our phenotyping platform.

These morphological adaptations translate into measurable relationships among the efficiency indicators, as shown by our PCA.

Correlations among phosphorus-efficiency indicators at harvest

Principal-component analysis (PCA) revealed a tight cluster comprising PAE and PUE, indicating that, under low-P conditions, plants that acquire more P also tend to convert it more efficiently into biomass. This co-variation was observed consistently across the experiment and matches results obtained after 96 days on a different phenotyping platform (ALSIA) (Sillo et

al. 2025), suggesting that wheat maintains a coordinated optimisation of acquisition and utilisation when P is limiting.

On the second principal component, PAE and PRAE (root-acquisition efficiency) showed a modest positive association, whereas PRAE and PUE were negatively correlated. This pattern implies that the ability of roots to acquire P per unit root biomass (PRAE) does not necessarily translate into higher P utilisation for growth. In other words, P use appears to depend more on traits other than simple root-biomass metrics – for instance, root metabolic activity, exudation profiles or microbial recruitment – rather than on the sheer amount of root tissue that explores the soil.

Deep phenotyping of root traits and their association with P-efficiency indicators

The high-throughput root-phenotyping platform allowed us to link dynamic root traits with the phosphorus-efficiency indicators (PAE, PRAE, PUE) defined in (Sillo et al. 2025). Traits that emerged as strong predictors of **PAE** and **PUE** - total root length, convex-hull area and root-length growth rate - are consistent with numerous reports that associate extensive root exploration with improved P uptake. This confirms that the phenotyping system can capture biologically meaningful variation under low-P conditions.

In contrast, **PRAE** showed little association with the morphometric variables measured. This likely reflects the involvement of processes that were not captured in the present experiment, such as root exudation of organic acids or phosphatases, activity of P-specific transporters (*e.g.*, PHT family), colonisation by arbuscular mycorrhizal fungi, or intracellular P-metabolism and remobilisation.

Future work should therefore include (i) high-resolution imaging of fine structures such as root hairs (using the high-resolution low-throughput cabin with ~7 µm resolution) and (ii) dedicated phenotyping of functional traits (exudate composition, microbial recruitment, transporter expression) to complete the picture of phosphorus acquisition.

Random-Forest analysis of dynamic trait parameters

This analysis identified total root length, root-growth rate, root convex-hull area and root density as the main traits associated with variation in both PAE and PUE. In contrast, SRR was retained only in the PAE model, despite the absence of a significant linear association with PAE. Its contribution may therefore reflect non-linear effects or interactions with other plant

traits rather than a direct effect of shoot-derived carbon allocation on root growth and P acquisition.

Gedser and *Bagou* were the highest- and lowest-performing genotypes, respectively. Their TRL_max_value and TRL_max_deriv traits were also the highest and less, respectively, correlated with PAE that demonstrates the importance of long and rapidly growing roots in the PAE efficiency to ensure plant growth performance.

Deep phenotyping allowed the characterization of phenotypic-trait dynamics between genotypes

The present study captured a larger set of root traits than previous work (Sillo et al. 2025) and tracked their dynamics throughout the growth period in RhizoTubes on the high-throughput phenotyping platform. The data confirm that wheat genotypes differ in their ability to acquire phosphorus (PAE, PRAE) and to use the absorbed P (PUE) by employing distinct root-system strategies. Overall, total root length, root density, convex-hull area and seminal root angle emerged as the key morphological descriptors linked to the phosphorus-efficiency indicators.

Accurate estimation of PUE is challenging because it is confounded by differences in P uptake (Rose et al. 2011) and differences in strategies of carbon allocation in shoot or root biomass among genotypes. By fixing the amount of P supplied *per* plant and by eliminating competition between individuals, the platform reduced the bias that typically inflates PUE estimates. Consequently, the results should be interpreted as relative acquisition and utilization strategies rather than as absolute PUE values. Validation of these observations will require complementary field trials that incorporate the heterogeneity of soil P availability and plant competition.

The contrasting root-length dynamics observed between the genotypes *Gedser* and *Bagou* illustrate this point. *Gedser* displayed a faster increase in root-exploration area (higher TRL_max_value and TRL_max_deriv values) and a larger total root biomass, which likely improved its capacity to harvest P from the substrate and to translocate it to the shoot, resulting in higher shoot biomass than *Bagou*. This suggests that, under a uniform low-P supply, expanding the soil surface explored by the root system can be more advantageous than increasing the efficiency of P uptake per unit root mass.

Root-system architecture and function are difficult to assess in the field because of soil heterogeneity, the complex wheat root structure and the logistical constraints of soil excavation (Degan et al. 2025). The high-throughput phenotyping approach therefore provides a valuable means to identify traits associated with phosphorus efficiency in large genotype panels. Traits such as total root length, fine-root density, exploration area, seminal-root angle and shoot-to-root ratio are central to acquisition strategies, yet they remain hard to measure under field conditions.

Heritability estimates confirmed that some dynamic parameters are under strong genetic control. The depth of the root centre of gravity (RGCY, $H^2 = 0.74$) and root density (RD, $H^2 = 0.71$) exhibited the highest broad-sense heritability, indicating that selection on these traits is feasible. By contrast, traits describing the horizontal gravity center (RGCX, RGCX80) showed low heritability because they mainly reflect lateral symmetry, which was limited in the experimental set-up.

When choosing phenotyping traits, researchers must balance feasibility, reproducibility, genetic variability, accuracy and biological relevance. For instance, PRAE was only weakly correlated with the measured morphometric variables (convex-hull area, root density), implying that additional mechanisms—such as root exudation, phosphate-transporter activity or mycorrhizal colonisation—drive this efficiency component. The current platform does not yet capture lateral-root number, spatial distribution, length or root-hair development; inclusion of these traits in future high-throughput systems would likely improve the explanatory power of the models.

Random-Forest analysis showed that total root length and convex-hull area were the most explanatory variables for PAE and PUE, whereas the studied morphometric traits exhibited only a very weak (if any) association with PRAE. Enhancing PRAE in genotypes that already exhibit high PAE and PUE could generate ideotypes that perform exceptionally under low-P conditions. To achieve this, functional traits—such as exudate composition, phosphatase activity or rhizosphere microbial recruitment—must be incorporated into phenotyping pipelines. Although progress is being made toward high-throughput measurement of these functional attributes, substantial technical challenges remain.

The physiological mechanisms underlying the identified traits, as well as the genes that control them, deserve further investigation. Previous work has shown that, under P limitation, the primary adaptive responses are increased root biomass and production of fine roots, whereas exudation of organic acids or phosphatases plays a secondary role (Shen et al. 2018). Mapping

quantitative trait loci (QTL) or expression-QTL (eQTL) for the high-heritability traits and linking them to candidate genes would enable marker-assisted selection for improved PAE and PUE. Manipulating genes involved in P metabolism, partitioning and redistribution has already been proposed as a route to boost PUE (Han et al. 2022).

Finally, the relevance of these findings must be confirmed under more realistic agronomic conditions. Controlled-environment experiments can be complemented with heterogeneous soil types, different P forms, and a broader set of genotypes to better mimic field complexity. Field phenotyping of root traits remains limited by destructive sampling and low throughput (Neumann et al. 2009), underscoring the continued importance of controlled platforms while emphasizing the need for automation to increase efficiency (Cabrera-Bosquet et al. 2026). Adjusting pot size, substrate composition and P diffusion rates (*e.g.*, by adding pre-absorbed P to activated alumina) could help replicate the slow P diffusion typical of soils and improve the transferability of results to the field (Da Silva and Gabelman 1992).

To refine the interpretation of these results, it is important to distinguish among the different processes that may underlie the observed variation in P efficiency. The observed differences in P efficiency should be interpreted cautiously, as they may reflect apparent efficiency, enhanced P acquisition capacity, or biomass-driven P uptake, rather than true differences in internal P utilization efficiency. This issue has been extensively discussed for nitrogen, where crop N uptake is known to be co-regulated by soil N availability, root distribution and plant growth capacity. Consequently, crop mass and plant nutritional status are considered key covariables for interpreting NUE across genotypes, environments and management conditions (Lemaire and Ciampitti 2020). A similar reasoning may apply to phosphorus. Genotypes with greater biomass may accumulate more P because of higher growth-driven P demand, leading to apparent differences in P efficiency that do not necessarily indicate improved internal P use. However, under the severe P deficiency imposed in the present study, differences in P efficiency may also arise from root traits and the ability to access poorly available P pools. Thus, the observed genotypic variation should be viewed as the result of interacting acquisition, growth and utilization processes, rather than attributed solely to internal P utilization efficiency. In this respect, root-phenotyping results obtained under controlled conditions would gain further relevance when evaluated alongside field data, as this would help determine whether root-system efficiency indicators are consistent with agronomic efficiency indicators derived from grain yield.

CONCLUSION

The high-throughput phenotyping platform employed in this study enables the measurement of root-morphometric traits that are difficult, or even impossible, to obtain in field experiments. Although the current suite of accessible traits is still limited, rapid methodological advances are expected to broaden the range of both morphological and functional root characteristics that can be captured at scale. To fully unravel the mechanisms underlying phosphorus-acquisition and use efficiency, the next step is to develop high-throughput phenotyping pipelines for root functional traits (exudate profiling, mycorrhizal colonisation, transporter activity). Combining these data with the current morphological descriptors will enable a more comprehensive ideotype definition for wheat adapted to low-P environments. These developments constitute a major asset for identifying genetically controlled traits linked to phosphorus acquisition and utilisation, and for defining phosphorus-efficient ideotypes (conceptual plant model combining target traits for a given environment) for wheat breeding.

Controlled-environment phenotyping and field trials should therefore be viewed as complementary (Cabrera-Bosquet et al. 2026): the former provides precision, repeatability and high throughput, while the latter offers agronomic relevance and captures environmental complexity. In the context of climate change, future work should integrate water-stress phenotyping to assess potential trade-offs between phosphorus capture and drought tolerance (*e.g.* (Ho et al. 2005)), thereby supporting the development of robust, climate-resilient wheat varieties.

Acknowledgments

We thank the Serres-4PMI staff of the platform (Plant Phenotyping Platform for Plant and Microorganisms Interactions) —UMR Agroécologie, Dijon, France for carrying out the experiment and the phenotypic analyses used in this work. We are most grateful to PLATIN' (Plateau d'Isotopie de Normandie) core facility for P analysis. We thank ARGO (INRAE) for its assistance in the linguistic review of this manuscript. ChatGPT (OpenAI) was used to assist in the graphical design of the experimental workflow (Figure 1), based on experimental information and reference photographs provided by the authors. The authors reviewed and validated the scientific content and final version of the figure. We would also like to thanks Chiara Pagliarani (IPSP Italy*)* for reviewing this version of the manuscript before its submission.

Funding

This work and financial support was provided through the project PGEN-BW (FSOV Project). We thank the Agence Nationale de la Recherche, Programme Investissements d'avenir, ANR-11-INBS-0012 (Phenome), which allowed us to acquire and run equipment within the 4PMI platform.

Declaration of competing interests

The authors declare that they have no known competing financial interests or personal relationships that could have appeared to influence the work reported in this paper.

Data availability

The data supporting the findings of this study are available in the table "Supplementary Supplementary_Table 1_Dataset.xlsx".

Author contributions:

Conceptualization, C.J. and C.S.; Data curation, C.J, C.S. and M.L.; Formal analysis, C.J. and C.S.; Funding acquisition, C.S.; Methodology, C.J, C.S. and M.L; Project administration, C.S.; Software, C.J. and M.L.; Supervision, C.S., C.J. and M.L.; Writing – original draft, C.S and C.J.; Writing – review and editing, C.S., C.J., F. D., F.S., R.B., M.L., M.P. All the authors read and approved the final manuscript.

REFERENCES

Bates TR, Lynch JP (2001) Root hairs confer a competitive advantage under low phosphorus availability. Plant and Soil. 236: 243-250.

Bradski G (2000) The OpenCV Library. Dr. Dobb's Journal of Software Tools. 25(11), 120–125. scikit-image

Cabrera-Bosquet L, Boureau T, Prudent M, Gardet R, Muller B (2026) Why bother with controlled-environment phenotyping when field phenomics is already up and running?, Journal of Experimental Botany, erag379, https://doi.org/10.1093/jxb/erag379

Da Silva A, Bruno IP, Franzini VI, Marcante NC, Benitiz L, Muraoka T (2016) Phosphorus uptake efficiency, root morphology and architecture in Brazilian wheat cultivars. Journal of Radioanalytical and Nuclear Chemistry. 307: 1055-1063.

Da Silva AE, Gabelman WH (1992) Screening maize inbred lines for tolerance to low-P stress condition. Plant and Soil. 146:1–2

Dawson CJ, Hilton J (2001) Fertilizer availability in a resource-limited world: production and recycling of nitrogen and phosphorus. Food Policy. 36: S14–S22.

Degan F, Creze, A, Salon C, Sillo F, Hawkesford M, Riche A, Bradley RS, Rollett A, Berry P, Wright T, et al. (2025) PGEN-BW. Phosphorus use efficiency and genetics of bread wheat (Déterminants génétiques de l'efficience d'utilisation du phosphore chez le blé tendre).

Dharmateja P, Kumar M, Pandey R, Mandal PK, Babu P, Bainsla NK, Gaikwad KB, Tomar V, Kranthi kumar K, Dhar N, et al (2021) Deciphering the change in root system architectural traits under limiting and non-limiting phosphorus in Indian bread wheat germplasm. PloS one. b(10), e0255840.

Dhillon J, Torres G, Driver E, Figueiredo B, Raun WR (2017) World phosphorus use efficiency in cereal crops. Agronomy Journal. 109: 1670-1677.

Fang Y, Lu L, Chen K, Wang X (2024) Tradeoffs among root functional traits for phosphorus acquisition in 13 soybean genotypes contrasting in mycorrhizal colonization. Annals of Botany. 134: 179–190.

Gahoonia T, Nielsen NE (2004) Root traits as tools for creating phosphorus-efficient crop varieties. Plant and Soil. 260: 47-57.

Han Y, White PJ, Cheng L (2022) Mechanisms for improving phosphorus utilization efficiency in plants. Annals of botany. 129(3), 247-258.

Heffer P (2013) Assessment of Fertilizer Use by Crop at the Global Level 2010–2010/11. International Fertilizer Association (IFA). https://www.fertilizer.org/resource/ assessment-of-fertilizer-use-by-crop-at-the-global- level-2010-2010-11.

Ho MD, Rosas JC, Brown KM, Lynch JP (2005) Root archi- tectural tradeoffs for water and phosphorus acquisition. Functional Plant Biology. 32:737–748

Jia XC, Liu P, Lynch JP (2018) Greater lateral root branching density in maize improves phosphorus acquisition from low phosphorus soil. Journal of Experimental Botany. 69: 4961–4970.

Jeudy C, Adrian M, Baussard C, Bernard C, Bernaud E, Bourion V, Busset H, Cabrera Bosquet LL, Cointault F, Han S, et al. (2016) RhizoTubes as a new tool for high throughput imaging of plant root development and architecture: test, comparison with pot-grown plants, and validation. Plant Methods. 12: 1-18.

Lambers H, Shane MW, Cramer MD, Pearse SJ, Veneklaas EJ (2006) Root structure and functioning for efficient acquisition of phosphorus: matching morphological and physiological traits. Annals of botany. 98(4), 693-713.

Lemaire G., Ciampitti I.A. (2020). Crop Mass and N Status as Prerequisite Covariables for Unraveling Nitrogen Use Efficiency across Genotype-by-Environment-by-Management Scenarios: A Review. Plants, 9, 1309. https://doi.org/10.3390/plants9101309

Li X, Chen Y, Xu Y, Sun H, Gao Y, Yan P, Song Q, Li S, Zhan A (2024) Genotypic variability in root morphology in a diverse wheat genotypes under drought and low phosphorus stress. Plants. 13: 3361.

Liaw A, Wiener M (2002) Classification and regression by randomForest. R news. 2:18–22.

Lynch JP (2007) Roots of the second green revolution. Australian Journal of Botany. 55(5), 493-512.

Marschner P, Crowley D, Rengel Z (2011) Rhizosphere interactions between microorganisms and plants govern iron and phosphorus acquisition along the root axis – model and research methods. Soil Biology and Biochemistry. 43: 883-894.

Maslard C, Arkoun M, Leroy F, Girodet S, Salon C and Prudent M (2026), Decoding the Double Stress Puzzle: Investigating Nutrient Uptake Efficiency and Root Architecture in Soybean Under Heat- and Water-Stresses. Plant, Cell & Environment, 49: 3710-3729. https://doi.org/10.1111/pce.15268

Millet EJ, Rodriguez-Alvarez MX, Perez Valencia DM, Sanchez I, Hilgert N, van Rossum BJ, van Eeuwijk FA, Boer M (2021). StatgenHTP: High throughput phenotyping (HTP) data analysis. R package version 1.0.5

Neumann G, George TS, Plassard C (2009) Strategies and methods for studying the rhizosphere. The plant science toolbox. Plant and Soil. 321: 431-456.

Nguyen VL, Stangoulis J (2019) Variation in root system architecture and morphology of two wheat genotypes as a predictor of their tolerance to phosphorus deficiency. Acta Physiologiae Plantarum. 41: 1-13.

Niu Y, Chai R, Jin G, Wang H, Tang C, Zhang Y (2013) Responses of root architecture development to low phosphorus availability: a review. Annals of Botany. 112:391–408

Pang JY, Bansal R, Zhao HX, Bohuon E, Lambers H, Ryan MH, Ranathunge K, Siddique KHM (2018) The carboxylate-releasing phosphorus-mobilizing strategy can be proxied by foliar manganese con- centration in a large set of chickpea germplasm under low phosphorus supply. New Phytologist. 219: 518–529.

R Core Team (2024) R: A language and environment for statistical computing. R Foundation for Statistical Computing, Vienna, Austria. https://www.R-project.org/

Roberts TL, Johnston AE (2015) Phosphorus use efficiency and management in agriculture. Resources, Conservation and Recycling. 105: 275-281.

Robles-Aguilar AA, Pang JY, Postma JA, Schrey SD, Lambers H, Jablonowski ND (2019) The effect of pH on morphological and physio- logical root traits of Lupinus angustifolius treated with struvite as a re- cycled phosphorus source. Plant and Soil. 434: 65–78.

Rose TJ, Rose MT, Pariasca-Tanaka J, Heuer S, Wissuwa M (2011) The frustration with utilization: why have improvements in internal phosphorus utilization efficiency in crops remained so elusive? Frontiers in Plant Science. 2, 73.

Shen Q, Wen Z, Dong Y, Li H, Miao Y, Shen J (2018) The responses of root morphology and phosphorus-mobilizing exudations in wheat to increasing shoot phosphorus concentration. AoB Plants. 10(5), ply054. https://doi.org/10.1093/aobpla/ply054.

Sillo F, Salon C, Lamboeuf M, Montesano V, Summerer S, Petrozza A, Conte A, Bergese F, Degan F, Balestrini R, et al. (2025) A novel P indicator to evaluate bread wheat (Triticum aestivum L.) genotypes to identify tolerance to phosphorus deficiency based on two distinct root phenotyping platforms. Annals of Botany. mcaf091.

Soumya PR, Vengavasi K, Pandey R (2022) Adaptive strategies of plants to conserve internal phosphorus under P deficient condition to improve P utilization efficiency. Physiology and Molecular Biology of Plants. 28(11), 1981-1993.

Sun BR, Gao YZ, Lynch JP (2018) Large crown root number improves top- soil foraging and phosphorus acquisition. Plant Physiology 177: 90–104.

Syers JK, Johnston AE, Curtin D (2008). Efficiency of soil and fertilizer phosphorus use: reconciling changing concepts of soil phosphorus behaviour with agronomic information. FAO Fertilizer and Plant Nutrition. Bulletin, 18. Rome: FAO.

Vance CP, Uhde-Stone C, Allan DL (2003) Phosphorus acquisition and use: critical adaptations by plants for securing a nonrenewable resource. New Phytologist. (2003). 157:423–447.

van der Walt S, Schönberger JL, Nunez-Iglesias J, Boulogne F, Warner JD, Yager N, Gouillart E, Yu T (2014). scikit-image: image processing in Python. PeerJ, 2, e453. https://doi.org/10.7717/peerj.453

Wang X, Shen J, Liao H (2010) Acquisition or utilization, which is more critical for enhancing phosphorus efficiency in modern crops?. Plant science. 179(4), 302-306.

Wang X, Pang J, Wen Z, Gadot G, de Borda A, Siddique KHM, Lambers H (2021) Lower seed P content does not affect early growth in chickpea, provided starter P fertiliser is supplied. Plant and Soil. 463(1), 113-124.

Wang W, Ding GD, White PJ, Wang XH, Jin KM, Xu FS, Shi L (2019) Mapping and cloning of quantitative trait loci for phosphorus efficiency in crops: opportunities and challenges. Plant and Soil. 439(1), 91-112.

Wen Z, Li H, Shen Q, Tang X, Xiong C, Li H, Pang J, Ryan MH, Lambers H, Shen J (2019) Tradeoffs among root morphology, exudation and mycorrhizal symbioses for phosphorus-acquisition strategies of 16 crop species. New Phytologist. 223(2), 882-895.

Yan X, Chen X, Ma C, et al., Zhang F (2021) What are the key factors affecting maize yield response to and agronomic efficiency of phosphorus fertilizer in China? Field Crops Research. 270, 108221.

Yan X, Liao H, Beebe SE, Blair MW, Lynch JP (2004) QTL mapping of root hair and acid exudation traits and their relationship to phosphorus uptake in common bean. Plant and Soil. 265:17–29.

Yang SY, Grønlund M, Jakobsen I, Grotemeyer MS, Rentsch D, Miyao A, Hirochika H, Kumar CH, Sundaresan V, Salamin S, et al. (2012) Nonredundant regulation of rice arbuscular mycorrhizal symbiosis by two members of the Phosphate Transporter gene family. The Plant Cell. 24(10), 4236-4251.

Yasrab R, Atkinson JA, Wells DM, French AP, Pridmore TP, Poung MP (2019) RootNav 2.0: Deep learning for automatic navigation of complex plant root architectures. GigaScience. 8(11), giz123.

Zhang L, Shi N, Fan JQ, Wang F, George TS, Feng G (2018) Arbuscular mycorrhizal fungi stimulate organic phosphate mobilization associated with changing bacterial community structure under field conditions. Environmental Microbiology. 20: 2639–2651.

Supplementary Files

This is a list of supplementary files associated with this preprint. Click to download.

- SupplementaryTable1Dataset.xlsx